High-Energy Scattering in QCD: Putting Together All the Main Ingredients

José Daniel Madrigal Martínez†

IPhT CEA-Saclay

Seminar at IFT UAM/CSIC
2 November 2015

† **Based on work in collaboration with E. Iancu, A.H. Mueller, G. Soyez and D.N. Triantafyllopoulos** [PLB**744** (2015) 293, PLB**750** (2015) 643 and work in progress]

High-Energy Scattering in QCD

Looking Inside the Nucleons

- Only 5 % of the mass of the universe is visible, but 99 % of this visible matter is described by QCD. This vast bulk of visible matter therefore comprises nontrivial emergent phenomena to be understood in terms of the rich dynamics of the QCD vacuum and the interactions of quarks and gluons.
- Subtle interplay between soft and hard dynamics makes high energy evolution very interesting.

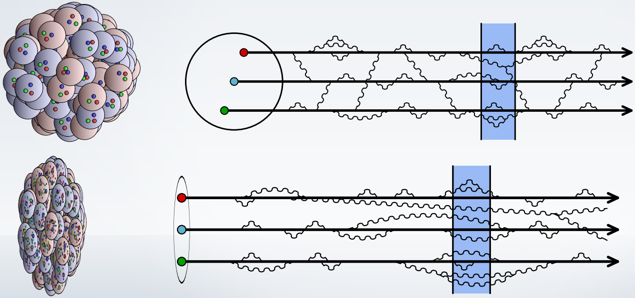

The Case of Deep-Inelastic Scattering

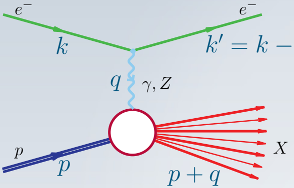

$$Q^2 = -q^2; \quad x_{\rm Bj} \simeq \frac{Q^2}{\hat{s}} = \frac{Q^2}{2p^- q^+}$$

Two important limits:

$Q^2, \hat{s} \to \infty; \quad x_{\rm Bj}$ fixed (Bjorken)

Q^2 fixed, $\hat{s} \to \infty; \quad x_{\rm Bj} \to 0$ (Regge)

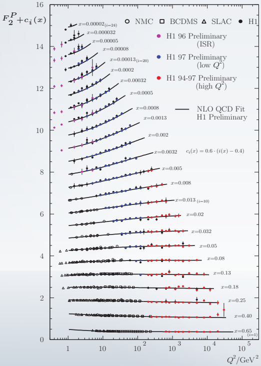

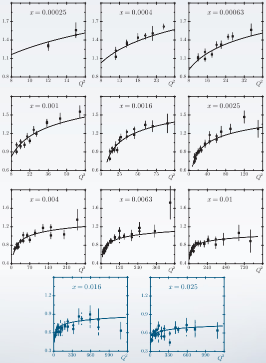

Gluon Bremsstrahlung and DGLAP Evolution

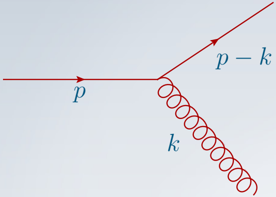

$$k_z = xp \gg k_\perp$$
$$0 < x < 1$$

$$dP_{\text{Brems}} \simeq \frac{\alpha_s \{C_A, C_F\}}{\pi^2} \frac{d^2 k_\perp}{k_\perp^2} \frac{dx}{x}$$

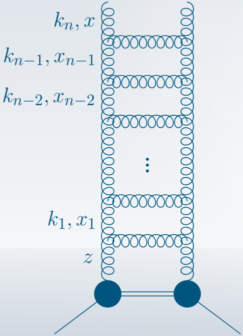

$$Q^2 \frac{\partial f_i(x, Q^2)}{\partial Q^2} = \frac{\alpha_s}{2\pi} \int_x^1 \frac{\mathrm{d}z}{z} P_{ji}\left(\frac{x}{z}\right) f_j\left(\frac{x}{z}, Q^2\right)$$

[Gribov & Lipatov ’72; Dokshitzer ’77; Altarelli & Parisi ’77]

Effectively resums ladder diagrams enhanced by transverse logs

$$Q_0^2 \ll \boldsymbol{k}_1^2 \ll \boldsymbol{k}_2^2 \ll \boldsymbol{k}_3^2 \ll \cdots$$
$$k_i^+ \simeq k_j^+ \Longrightarrow k_1^- \ll k_2^- \ll k_3^- \ll \cdots$$

Large Energy Logs Enter the Game

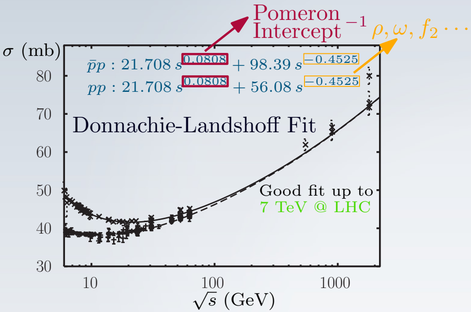

Mild power rise of total hadronic cross-section in semi-asymptotic regime

[Donnachie & Landshoff '90]

$\sim$ means *as* $s \to \infty$

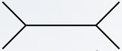

$A^{(1)} \sim \frac{g^2}{s}$

$A^{(2)} \sim \frac{g^2}{s} K(t) \ln s$

$K(t) \sim g^2 \int \frac{d^2\mathbf{k}_\perp}{(\mathbf{k}_\perp^2 + m^2)[(\mathbf{k}_\perp + \mathbf{q}_\perp)^2 + m^2]}$

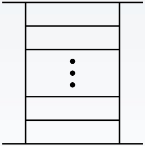

$A^{(n)} \sim \frac{g^2}{s} \frac{(K(t) \ln s)^{n-1}}{(n-1)!}$

$$A(s,t) = \sum_{n=1}^{\infty} A^{(n)} \sim \sum_{n=1}^{\infty} \frac{g^2}{s} \frac{(K(t)\ln s)^{n-1}}{(n-1)!} \simeq \frac{g^2}{s} e^{K(t)\ln s} \simeq g^2 s^{\alpha(t)}$$

High-Energy Evolution: the Russian Approach

Corrections to Born Scattering

- **Virtual** ($\mathbf{8}_a$ Projected)

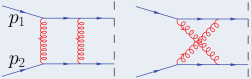

$$\simeq \text{Born} \times \omega(\boldsymbol{q}^2) \ln \frac{s}{s_0}$$

$$\omega(\boldsymbol{q}^2) = -\frac{g^2 N_c}{8\pi^2} \ln \frac{\boldsymbol{q}^2}{\mu^2}$$

- **Real** (Lipatov's Vertex)

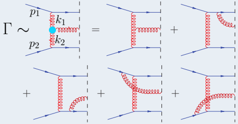

$$\int d\Pi \, \Gamma\Gamma^* \sim \ln \frac{s}{s_0}$$

IR singularities cancel

High-Energy Factorization

$$A^{\mathrm{MRK}}_{2\to 2+n} = A^{\mathrm{tree}}_{2\to 2+n} \prod_{i=1}^{n+1} s_i^{\omega(t_i)}, \qquad A^{\mathrm{tree}}_{2\to 2+n} = 2gsT^{c_1}_{A'A}$$

$$\times \Gamma_1 \frac{1}{t_1} g T^{d_1}_{c_2 c_1} \Gamma^1_{2,1} \frac{1}{t_2} \cdots g T^{d_n}_{c_{n+1} c_n} \Gamma^n_{n+1,n} \frac{1}{t_{n+1}} g T^{c_{n+1}}_{B'B} \Gamma_2$$

Lipatov's Ansatz

[Lipatov'76]

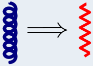

$$\frac{-i}{k_i^2} \to \frac{-i}{k_i^2}\left(-\frac{s_i}{k_i^2}\right)^{\alpha(-k_i^2)}$$

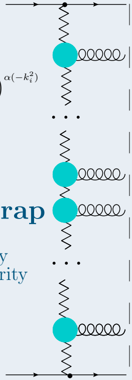

The ansatz satisfies

- ☐ **Bootstrap**
- ☐ Consistency with Unitarity

Leading $\ln s$ terms captured by strong ordering in rapidity

The BFKL Equation

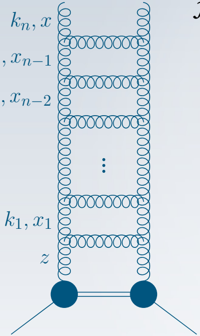

$$\mathcal{F}(x,Q^2)=\mathcal{F}^{(0)}(x,Q^2)+\int\frac{\mathrm{d}z}{z}\int\mathrm{d}\boldsymbol{k}^2\mathcal{K}_{\mathrm{BFKL}}(Q^2,\boldsymbol{k}^2)\mathcal{F}\left(\frac{x}{z},\boldsymbol{k}^2\right)$$

$$g(x,Q^2)\equiv\int\frac{\mathrm{d}^2\boldsymbol{k}}{\pi\boldsymbol{k}^2}\Theta(Q^2-\boldsymbol{k}^2)\mathcal{F}(x,\boldsymbol{k}^2);$$

$$\mathcal{K}_{\mathrm{BFKL}}=\bar{\alpha}_s\left[\frac{1}{(\boldsymbol{Q}-\boldsymbol{k})^2}-\delta(Q^2-\boldsymbol{k}^2)\int^{\boldsymbol{k}}\frac{\mathrm{d}^2\boldsymbol{q}}{\pi\boldsymbol{q}^2}\right]$$

[Fadin, Kuraev & Lipatov '75,76,77; Lipatov'76; Balitsky & Lipatov '78]

$$q^+>k_1^+\gg k_2^+\gg k_3^+\gg\cdots$$
$$Q_0^2\simeq\boldsymbol{k}_1^2\simeq\boldsymbol{k}_2^2\simeq\boldsymbol{k}_3^2\simeq\cdots$$

- Multi-Regge-kinematics not satisfied in all regions of transverse integration
- Pay attention to evolution variable! $Y=\ln\left(\frac{k^+}{q^+}\right)=\ln\left(\frac{x_0}{x_{\mathrm{Bj}}}\frac{Q^2}{Q_0^2}\right)$

The Interplay Between DGLAP and BFKL Evolutions

Powers resummed up to n^{th} perturbative order by

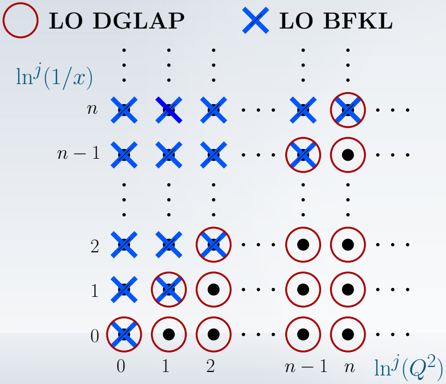

Connections Between Collinear and Regge-Limit Expansions

- One can use one expansion to predict the leading log terms in the other expansion in a certain limit:
  - BFKL→DGLAP
    [Jaroszewicz'82; Catani, Fiorani & Marchesini'90]
  - DGLAP→BFKL
    [Salam'98; Altarelli, Ball & Forte'00; Kotikov & Lipatov'03; Balitsky, Kazakov & Sobko'13]ç
- This connection has also been extended to strong coupling:
  [Kotikov, Lipatov, Rej, Staudacher & Velizhanin'07; Hatta, Iancu & Mueller'07; Staśto'07; Kotikov & Lipatov'13]

Mind the Anomalous Dimension

It is convenient to diagonalize the evolution equation via Mellin transform ($\rho = \ln \frac{Q^2}{Q_0^2}$)

$$\mathcal{F}(\rho, Y) = \int \frac{\mathrm{d}\omega}{2\pi \mathrm{i}} \mathrm{e}^{\omega Y} \int \frac{\mathrm{d}\gamma}{2\pi \mathrm{i}} \mathrm{e}^{-\rho\gamma} \hat{\mathcal{F}}(\gamma, \omega)$$

$$\hat{\mathcal{F}}(\gamma, \omega) = \frac{\hat{\mathcal{F}}^0(\gamma)}{\omega - \bar{\alpha}_s \chi(\gamma)}, \quad \chi(\gamma) = 2\psi(1) - \psi(\gamma) - \psi(1-\gamma)$$

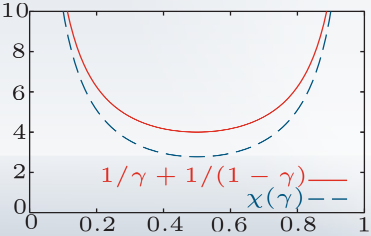

$$\gamma_\omega = \lambda + 0\lambda^2 + 0\lambda^3 + 2\zeta_3\lambda^4 + \mathcal{O}(\lambda^6),$$

$$\lambda = \frac{\alpha_s N_c}{\pi\omega}$$

[Jaroszewicz'82]

The Kinematic Map of QCD

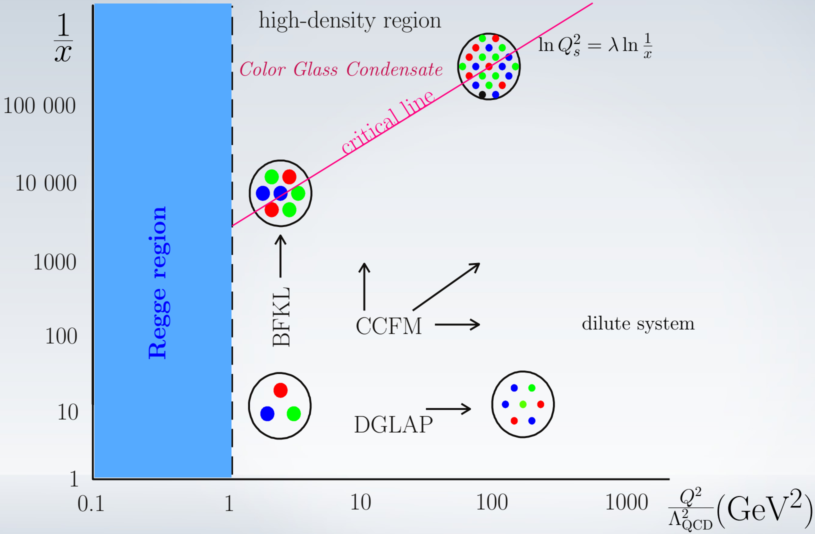

Why All the Fuss About Small-x

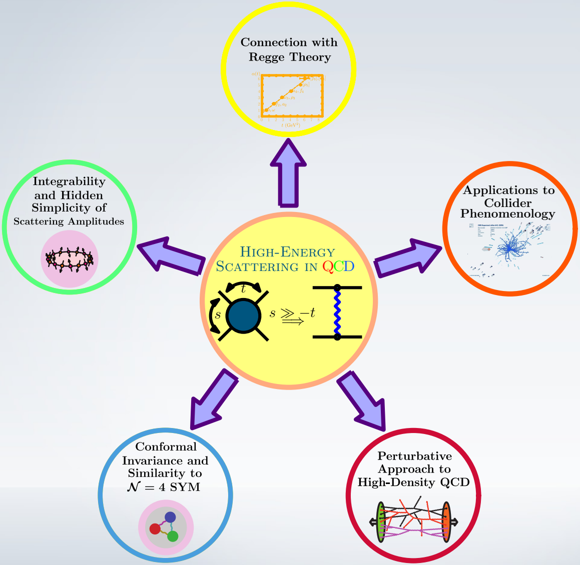

Disentangling High-Energy Dynamics at LHC

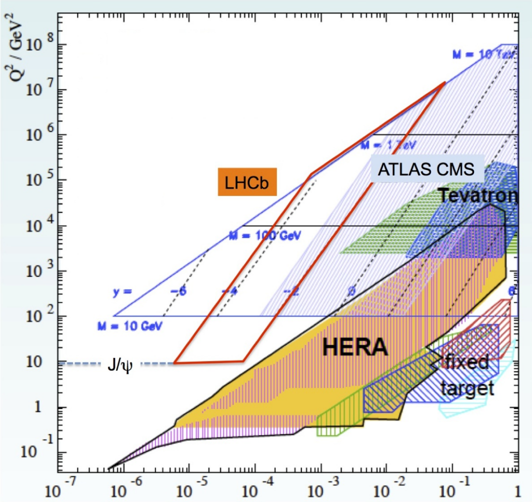

CERN-PH-LPCC-2015-001
SLAC-PUB-16364
DESY 15-167

September 3 2015

LHC Forward Physics

Editors: N. Cartiglia, C. Royon
The LHC Forward Physics Working Group

K. Akiba[21], M. Akbiyik[1], M. Albrow[2], M. Arneodo[3,4], V. Avati[5,6], J. Baechler[6], O. Villalobos Baillie[87], P. Bartalini[7], J. Bartels[8], S. Baur[1], C. Baus[1], W. Beaumont[9], U. Behrens[10], D. Berge[11], M. Berretti[6,12], E. Bossini[12], R. Boussarie[13], S. Brodsky[14], M. Broz[15], M. Bruschi[16], P. Bussey[17], W. Byczynski[81], J. C. Cabanillas Noris[18], E. Calvo Villar[19], A. Campbell[10], F. Caporale[22], W. Carvalho[21], G. Chachamis[22], E. Chapon[23], C. Cheshkov[24], J. Chwastowski[25], R. Ciesielski[26], D. Chinellato[83], A. Cisek[25], V. Coco[6], P. Collins[6], J. G. Contreras[15], B. Cox[27], D. de Jesus Damiao[21], P. Davis[28], M. Deile[6], D. D'Enterria[6], D. Druzhkin[29,6], B. Ducloué[30,31], R. Dumps[6], R. Dzhelyadin[82] P. Dziurdzia[6], M. Eliachevitch[1], P. Fassnacht [6] F. Ferro[32], S. Fichet[33], D. Figueiredo[21], B. Field[34], D. Finogeev[35], R. Fiore[29,36], J. Forshaw[27], A. Gago Medina[19], M. Gallinaro[37], A. Granik[82], G. von Gersdorff[33], S. Giani[6], K. Golec-Biernat[25,38], V. P. Goncalves[39], P. Göttlicher[10], K. Goulianos[26], J.-Y. Grosslord[24], L. A. Harland-Lang[40], H. Van Haevermaet[9], M. Hentschinski[41], R. Engel [1], G. Herrera Corral[42], J. Hollar[37], L. Huertas[21], D. Johnson[6], I. Katkov[1], O. Kepka[43], M. Khakzad[44], L. Kheyn[45], V. Khachatryan[46], V. A. Khoze[47], S. Klein[48], M. van Klundert[9], F. Krauss[47], A. Kurepin[35], N. Kurepin[35], K. Kutak[49], E. Kuznetsova[1], G. Latino[12], P. Lebiedowicz[25], B. Lenzi[6], E. Lewandowska[25], S. Liu[28], A. Luszczak[25,38], M. Luszczak[25], J. D. Madrigal[50], M. Mangano[6], Z. Marcone[34], C. Marquet[51], A. D. Martin[47], T. Martin[52], M. I. Martinez Hernandez[53], C. Martins[21], C. Mayer[25], R. Mc Nulty[54], P. Van Mechelen[7], R. Macula[25], E. Melo da Costa[21], T. Mertzimekis[55], C. Mesropian[26], M. Mieskolainen[31], N. Minafra[6,56], I. L. Monzon[18], L. Mundim [21], B. Murdaca[20,36], M. Murray[57], H. Niewiadowski[58], J. Nystrand[59], E. G. de Oliveira[60], R. Orava[31], S. Ostapchenko[61], K. Osterberg[31], A. Panagiotou[55], A. Papa[20], R. Pasechnik[62], T. Peitzmann[63], L. A. Perez Moreno[53], T. Pierog[1], J. Pinfold[28], M. Poghosyan[64], M. E. Pol[65], W. Prado[21], V. Popov[66], M. Rangel[67], A. Reshetin[35], J.-P. Revol[68], M. Rijssenbeek[34], M. Rodriguez [5]3, B. Roland[10], C. Royon[25,43,57], M. Ruspa[3,4], M. Ryskin[47,69], A. Sabio Vera[22], G. Safronov[66], T. Sako[70], H. Schindler[6], D. Salek[11], K. Safarik [6], M. Saimpert[71], A. Santoro[21], R. Schicker[73], J. Seger[64], S. Sen[73], A. Shabanov[35], W. Schafer[25], G. Gil Da Silveira[39], P. Skands[74], R. Soluk[28], A. van Spilbeeck[9], R. Staszewski[25], S. Stevenson[75], J. Stirling[86], M. Strikman[76], A. Szczurek[25,38] L. Szymanowski[77], J.D. Tapia Takaki,[57] M. Tasevsky[43], K. Taesoo[78], C. Thomas[75], S. R. Torres[18], A. Tricomi[79], M. Trzebinski[25], D. Tsybychev[34], N. Turini[12], R. Ulrich[1], E. Usenko[35], J. Varela[37], M. Lo Vetere[80], A. Villatoro Tello[53], A. Vilela Pereira[21], D. Volyanskyy [84], S. Wallon[13,85], G. Wilkinson[75], H. Wöhrmann[1]. K. C. Zapp[6], Y. Zoccarato[24].

[1] *Karlsruhe Institute of Technology (KIT), Karlsruhe, Germany*
[2] *Fermilab, Batavia, USA*
[3] *INFN Torino, Italy*
[4] *Universitá del Piemonte Orientale, Novara, Italy*
[5] *AGH University of Science and Technology, Krakow, Poland*
[6] *CERN, Geneva, Switzerland*
[7] *Central China Normal University (CCNU), Wuhan, Hubei, China*
[8] *University of Hamburg, Germany*
[9] *University of Antwerpen, Belgium*
[10] *DESY, Hamburg, Germany*
[11] *NIKHEF and GRAPPA, Amsterdam, Netherlands*
[12] *INFN Pisa, Pisa, Italy and Universita degli Studi di Siena, Siena, Italy*
[13] *LPT, Université Paris-Sud, CNRS, 91405, Orsay, France*
[14] *SLAC National Accelerator Laboratory, Stanford University, Stanford, CA, USA*
[15] *Faculty of Nuclear Sciences and Physical Engineering, Czech Technical University in Prague, Prague, Czech Republic*

Towards Saturation: Eikonal Scattering and the Dipole Picture

- At very high energies the scattering of a fast projectile is given by the eikonal approximation: it amounts to picking up a phase given by the Wilson line $\boldsymbol{U_x = \mathcal{P}\mathrm{exp}\left[\mathrm{i}g\int \mathrm{d}x^+ A_a^-(x^+, x)T^a\right]}$

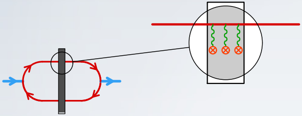

Dipole Scattering Amplitude

$$\mathcal{T} = 1 - S$$

$$S_{\boldsymbol{xy}} = \frac{1}{N_c}\mathrm{Tr}(U_{\boldsymbol{x}}U_{\boldsymbol{y}}^{\dagger})$$

$$\propto \Psi_{ij}^{(0)*}(\boldsymbol{x},\boldsymbol{y})\Psi_{kl}^{(0)}(\boldsymbol{x},\boldsymbol{y})U_{ik}(\boldsymbol{x})U_{lj}^{\dagger}(\boldsymbol{y}) \propto |\Psi^{(0)}(\boldsymbol{x},\boldsymbol{y})|^2 S_{\boldsymbol{xy}}$$

- Mixed representation $\{x_\perp, k^+\}$ well-suited for high-energy scattering (diagonalizes shockwave interaction)

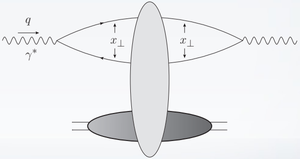

Dipole Factorization

[Nikolaev & Zakharov '91; Mueller '94]

The Balitsky-Kovchegov Equation

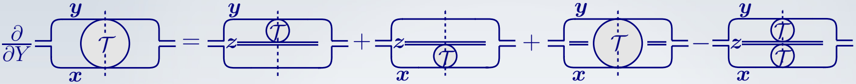

Balitsky-Kovchegov (BK) equation

$$\partial_Y T_{\boldsymbol{xy}} = -\frac{\bar{\alpha}_s}{2\pi} \int_{\boldsymbol{z}} \mathcal{M}_{\boldsymbol{xyz}} [T_{\boldsymbol{xz}} + T_{\boldsymbol{zy}} - T_{\boldsymbol{xy}} - T_{\boldsymbol{xz}} T_{\boldsymbol{zy}}];$$

$$\mathcal{M}_{\boldsymbol{xyz}} = \frac{(\boldsymbol{x}-\boldsymbol{y})^2}{(\boldsymbol{x}-\boldsymbol{z})^2 (\boldsymbol{z}-\boldsymbol{y})^2}$$

[Balitsky '96; Kovchegov '98]

- Tames the Growth: Saturation
- Generates dynamical perturbative scale Q_s
- Geometric Scaling

Beyond BK

Balitsky-Kovchegov equation also emerges as mean-field-approximation of **JIMWLK formalism**

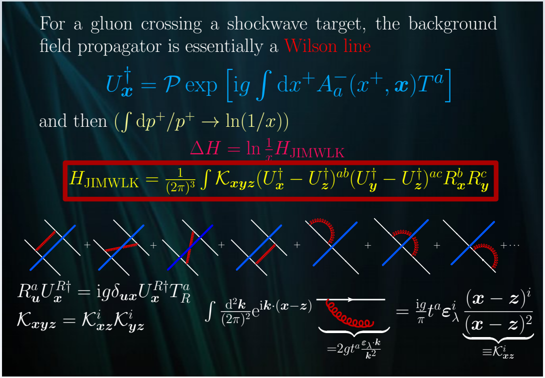

[Jalilian-Marian, Kovner, McLerran & Weigert '97; Iancu, Leonidov & McLerran '01]

Actually, BK and JIMWLK predictions for dipole scattering amplitude turn out to be very similar [Kuokkanen, Rummukainen & Weigert '08]

The Issue with NLO Corrections

- *Tour-de-force* computations of NLO corrections to BFKL [Fadin & Lipatov '98; Camici & Ciafaloni '98], BK [Balitsky & Chirilli '08] and JIMWLK [Balitsky & Chirilli '13; Kovner, Lublinsky & Mulian '14] equations. NLO accuracy indispensible for sensible phenomenology.
- Large size of the NLO corrections found in BFKL equation, that would deprive it of its predictive power and lead to instabilities [Ross '98].

The Issue with NLO Corrections

- *Tour-de-force* computations of NLO corrections to BFKL [Fadin & Lipatov '98; Camici & Ciafaloni '98], BK [Balitsky & Chirilli '08] and JIMWLK [Balitsky & Chirilli '13; Kovner, Lublinsky & Mulian '14] equations. NLO accuracy indispensible for sensible phenomenology.
- Large size of the NLO corrections found in BFKL equation, that would deprive it of its predictive power and lead to instabilities [Ross '98].
- No reason to expect lack-of-convergence problems to be attenuated by non-linear terms in BK-JIMWLK equation [Triantafyllopoulos '03; Avsar, Staśto, Triantafyllopoulos & Zaslavsky '11].

The Issue with NLO Corrections

- *Tour-de-force* computations of NLO corrections to BFKL [Fadin & Lipatov '98; Camici & Ciafaloni '98], BK [Balitsky & Chirilli '08] and JIMWLK [Balitsky & Chirilli '13; Kovner, Lublinsky & Mulian '14] equations. NLO accuracy indispensible for sensible phenomenology.
- Large size of the NLO corrections found in BFKL equation, that would deprive it of its predictive power and lead to instabilities [Ross '98].
- No reason to expect lack-of-convergence problems to be attenuated by non-linear terms in BK-JIMWLK equation [Triantafyllopoulos '03; Avsar, Staśto, Triantafyllopoulos & Zaslavsky '11].
- Origin of large NLO corrections identified to come from large transverse logarithms. Several procedures devised for all-order resummation of large logs and stabilization of the kernel [Salam '98; Ciafaloni, Colferai, Salam & Staśto '03; Sabio Vera '05].

The Issue with NLO Corrections

- *Tour-de-force* computations of NLO corrections to BFKL [Fadin & Lipatov '98; Camici & Ciafaloni '98], BK [Balitsky & Chirilli '08] and JIMWLK [Balitsky & Chirilli '13; Kovner, Lublinsky & Mulian '14] equations. NLO accuracy indispensible for sensible phenomenology.
- Large size of the NLO corrections found in BFKL equation, that would deprive it of its predictive power and lead to instabilities [Ross '98].
- No reason to expect lack-of-convergence problems to be attenuated by non-linear terms in BK-JIMWLK equation [Triantafyllopoulos '03; Avsar, Staśto, Triantafyllopoulos & Zaslavsky '11].
- Origin of large NLO corrections identified to come from large transverse logarithms. Several procedures devised for all-order resummation of large logs and stabilization of the kernel [Salam '98; Ciafaloni, Colferai, Salam & Staśto '03; Sabio Vera '05].

Double Transverse Logs in BK

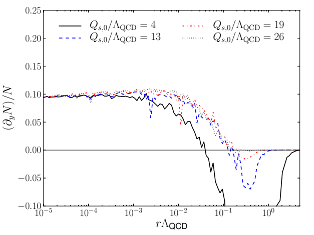

(a) $\gamma = 0.6$

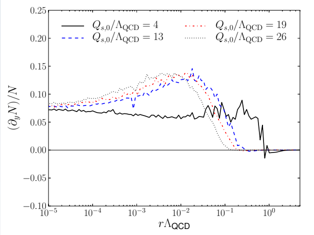

(b) $\gamma = 0.8$

Large corrections and instabilities in NLO BK traced back to double transverse logs [Lappi & Mantysäari '15]:

$$\begin{aligned}
\frac{d}{d\eta}\,\mathrm{Tr}\{\hat U_x \hat U_y^\dagger\} = \frac{\alpha_s}{2\pi^2}\int d^2z\,\frac{(x-y)^2}{X^2Y^2}\Big\{1 + \frac{\alpha_s}{4\pi}\Big[b\ln(x-y)^2\mu^2 - b\,\frac{X^2-Y^2}{(x-y)^2}\ln\frac{X^2}{Y^2} + \Big(\frac{67}{9}-\frac{\pi^2}{3}\Big)N_c - \frac{10}{9}n_f \\
- 2N_c\ln\frac{X^2}{(x-y)^2}\ln\frac{Y^2}{(x-y)^2}\Big]\Big\}\big[\mathrm{Tr}\{\hat U_x\hat U_z^\dagger\}\,\mathrm{Tr}\{\hat U_z\hat U_y^\dagger\} - N_c\,\mathrm{Tr}\{\hat U_x\hat U_y^\dagger\}\big] \\
+ \frac{\alpha_s^2}{16\pi^4}\int d^2z\,d^2z'\Big[\Big(-\frac{4}{(z-z')^4} + \Big\{2\,\frac{X^2Y'^2 + X'^2Y^2 - 4(x-y)^2(z-z')^2}{(z-z')^4[X^2Y'^2 - X'^2Y^2]} + \frac{(x-y)^4}{X^2Y'^2 - X'^2Y^2} \\
\times\Big[\frac{1}{X^2Y'^2} + \frac{1}{Y^2X'^2}\Big] + \frac{(x-y)^2}{(z-z')^2}\Big[\frac{1}{X^2Y'^2} - \frac{1}{X'^2Y^2}\Big]\Big\}\ln\frac{X^2Y'^2}{X'^2Y^2}\Big)\big[\mathrm{Tr}\{\hat U_x\hat U_z^\dagger\}\,\mathrm{Tr}\{\hat U_z\hat U_{z'}^\dagger\}\,\mathrm{Tr}\{\hat U_{z'}\hat U_y^\dagger\} \\
- \mathrm{Tr}\{\hat U_x\hat U_z^\dagger\hat U_{z'}U_y^\dagger\hat U_z\hat U_{z'}^\dagger\} - (z'\to z)\big] + \Big\{\frac{(x-y)^2}{(z-z')^2}\Big[\frac{1}{X^2Y'^2} + \frac{1}{Y^2X'^2}\Big] - \frac{(x-y)^4}{X^2Y'^2X'^2Y^2}\Big\}\ln\frac{X^2Y'^2}{X'^2Y^2} \\
\times\mathrm{Tr}\{\hat U_x\hat U_z^\dagger\}\,\mathrm{Tr}\{\hat U_z\hat U_{z'}^\dagger\}\,\mathrm{Tr}\{\hat U_{z'}\hat U_y^\dagger\} + 4n_f\Big\{\frac{4}{(z-z')^4} - 2\,\frac{X'^2Y^2 + Y'^2X^2 - (x-y)^2(z-z')^2}{(z-z')^4(X^2Y'^2 - X'^2Y^2)}\ln\frac{X^2Y'^2}{X'^2Y^2}\Big\}
\end{aligned}$$

The Goals of Our Work

1. Identify the diagrammatic origin of double logarithmic corrections and its relation to the 'kinematic constraint'

   [Ciafaloni '88; Andersson, Gustafson & Samuelsson '96; Kwieciński, Martin & Sutton '96; Beuf '14].

2. Implement directly the collinear resummation in coordinate space, as required by non-linear structure of BK equation.

The Goals of Our Work

1. Identify the diagrammatic origin of double logarithmic corrections and its relation to the 'kinematic constraint' [Ciafaloni '88; Andersson, Gustafson & Samuelsson '96; Kwieciński, Martin & Sutton '96; Beuf '14].
2. Implement directly the collinear resummation in coordinate space, as required by non-linear structure of BK equation.
3. Express the resummed evolution equation in terms of a local (energy-independent) kernel, as compared to non-local in rapidity proposals [Motyka & Staśto '09; Beuf '14]

The Goals of Our Work

1. Identify the diagrammatic origin of double logarithmic corrections and its relation to the 'kinematic constraint' [Ciafaloni '88; Andersson, Gustafson & Samuelsson '96; Kwieciński, Martin & Sutton '96; Beuf '14].
2. Implement directly the collinear resummation in coordinate space, as required by non-linear structure of BK equation.
3. Express the resummed evolution equation in terms of a local (energy-independent) kernel, as compared to non-local in rapidity proposals [Motyka & Staśto '09; Beuf '14]
4. Show the relevance of our collinear resummation for BK equation studying its numerical solution and precision fits to DIS data.

The Goals of Our Work

1. Identify the diagrammatic origin of double logarithmic corrections and its relation to the 'kinematic constraint' [Ciafaloni '88; Andersson, Gustafson & Samuelsson '96; Kwieciński, Martin & Sutton '96; Beuf '14].
2. Implement directly the collinear resummation in coordinate space, as required by non-linear structure of BK equation.
3. Express the resummed evolution equation in terms of a local (energy-independent) kernel, as compared to non-local in rapidity proposals [Motyka & Staśto '09; Beuf '14]
4. Show the relevance of our collinear resummation for BK equation studying its numerical solution and precision fits to DIS data.

The Origin of Double Logs

(Naive) DLA Limit of the BFKL Equation

BFKL Equation $(T = 1 - S, T \ll 1)$

$$\partial_Y T_{\boldsymbol{xy}}(Y) = \frac{\bar{\alpha}_s}{2\pi} \int \mathrm{d}^2\boldsymbol{z} \mathcal{M}_{\boldsymbol{xyz}} [T_{\boldsymbol{xz}}(Y) + T_{\boldsymbol{zy}}(Y) - T_{\boldsymbol{xy}}(Y)]$$

$\boldsymbol{z}$-integration becomes logarithmic when daughter dipoles are much larger than the original one $(|\boldsymbol{x} - \boldsymbol{z}| \simeq |\boldsymbol{z} - \boldsymbol{y}| \gg r \equiv |\boldsymbol{x} - \boldsymbol{y}|)$

$\mathcal{M}_{\boldsymbol{xyz}} \simeq r^2/(\boldsymbol{x} - \boldsymbol{z})^4$ and $T_{\boldsymbol{xz}} \simeq T_{\boldsymbol{zy}} \propto \boldsymbol{z}^2$; negligible virtual term.

Writing $T_{\boldsymbol{xy}}(Y) \equiv r^2 Q_0^2 \mathcal{A}_{\boldsymbol{xy}} \to r^2 Q_0^2 \mathcal{A}(Y, r^2)$

$$\mathcal{A}(Y, r^2) = \mathcal{A}(0, r^2) + \bar{\alpha}_s \int_0^Y \mathrm{d}Y_1 \int_{r^2}^{1/Q_0^2} \frac{\mathrm{d}z^2}{z^2} \mathcal{A}(Y_1, z^2)$$

(Naive) DLA Equation (resums powers of $\bar{\alpha}_s Y \rho$, $\rho \equiv \ln[1/r^2 Q_0^2]$ to all orders)

$$\mathcal{A}(Y, \rho) = I_0(2\sqrt{\bar{\alpha}_s Y \rho})$$

Computation of Time-Ordered Diagrams

- Lifetime of gluon fluctuation $\tau_p \equiv 2p^+/\boldsymbol{p}^2 = 1/p^-$
- Eikonal approximation $p^+ \gg k^+$

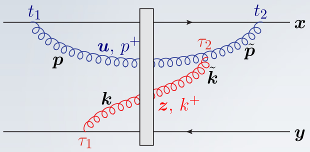

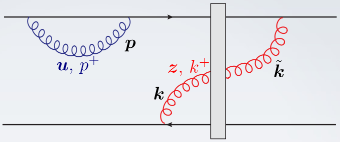

$$
-\frac{g^4 N_c^2}{(2\pi)^2}\int_{\boldsymbol{uz}} S_{\boldsymbol{xu}} S_{\boldsymbol{uz}} S_{\boldsymbol{zy}}
\times \int_{\boldsymbol{p}\tilde{\boldsymbol{p}}\boldsymbol{k}\tilde{\boldsymbol{k}}} e^{i\boldsymbol{p}\cdot(\boldsymbol{u}-\boldsymbol{x})} e^{i\tilde{\boldsymbol{p}}\cdot(\boldsymbol{x}-\boldsymbol{u})} e^{i\boldsymbol{k}\cdot(\boldsymbol{z}-\boldsymbol{y})} e^{i\tilde{\boldsymbol{k}}\cdot(\boldsymbol{u}-\boldsymbol{z})} \frac{\boldsymbol{p}\cdot\tilde{\boldsymbol{p}}}{\boldsymbol{p}^2\tilde{\boldsymbol{p}}^2}\frac{\boldsymbol{k}\cdot\tilde{\boldsymbol{k}}}{\boldsymbol{k}^2\tilde{\boldsymbol{k}}^2}
\times \int_{q_0^+}^{q^+}\frac{dk^+}{k^+}\int_{k^+}^{q^+}\frac{dp^+}{p^+}\boxed{\frac{p^+}{p^+ + k^+\frac{\boldsymbol{p}^2}{\boldsymbol{k}^2}}\ \frac{p^+}{p^+ + k^+\frac{(\tilde{\boldsymbol{p}}-\tilde{\boldsymbol{k}})^2}{\tilde{\boldsymbol{k}}^2}}}.
$$

$$
\frac{p^+}{p^+ + k^+\frac{\boldsymbol{p}^2}{\boldsymbol{k}^2}} = \frac{\tau_p}{\tau_p + \tau_k}
\simeq \begin{cases} 1 & \text{in BFKL} \\ \Theta(\tau_p - \tau_k) & \text{in DLA} \end{cases}
$$

Real-Real Contribution

$$\left(\frac{\bar{\alpha}_s}{2\pi}\right)^2 \int_{q_0^+}^{q^+} \frac{\mathrm{d}k^+}{k^+} \int_{k^+}^{q^+} \frac{\mathrm{d}p^+}{p^+} \int_{\boldsymbol{uz}} \mathcal{M}_{\boldsymbol{xyu}} [\mathcal{M}_{\boldsymbol{uyz}} S_{\boldsymbol{xu}} S_{\boldsymbol{uz}} S_{\boldsymbol{zy}} + \mathcal{M}_{\boldsymbol{xuz}} S_{\boldsymbol{xz}} S_{\boldsymbol{zu}} S_{\boldsymbol{uy}}]$$

$$\times \Theta(p^+ \bar{u}^2 - k^+ \bar{z}^2), \qquad \bar{u} = \max(|\boldsymbol{u} - \boldsymbol{x}|, |\boldsymbol{u} - \boldsymbol{y}|); \;\; \bar{z} = \max(|\boldsymbol{z} - \boldsymbol{x}|, |\boldsymbol{z} - \boldsymbol{y}|)$$

Virtual-Real Contribution

$$-\left(\frac{\bar{\alpha}_s}{2\pi}\right)^2 \int_{q_0^+}^{q^+} \frac{\mathrm{d}k^+}{k^+} \int_{k^+}^{q^+} \frac{\mathrm{d}p^+}{p^+} \int_{\boldsymbol{uz}} \mathcal{M}_{\boldsymbol{xyu}} \mathcal{M}_{\boldsymbol{xyz}} S_{\boldsymbol{xz}} S_{\boldsymbol{zy}} \Theta(p^+ \bar{u}^2 - k^+ \bar{z}^2)$$

To DLA accuracy $\mathcal{M}_{\boldsymbol{uyz}} \mathcal{M}_{\boldsymbol{xyu}} \simeq \frac{r^2}{\bar{u}^2 \bar{z}^4}$ and $1 - S_{\boldsymbol{xu}} S_{\boldsymbol{uz}} S_{\boldsymbol{zy}} \simeq T_{\boldsymbol{uz}} + T_{\boldsymbol{zy}} \simeq 2T(\bar{z}^2)$ and we generate logarithmic phase space

$$\int_{r^2}^{\bar{z}^2} \frac{\mathrm{d}\bar{u}^2}{\bar{u}^2} \int_{k^+ \frac{\bar{z}^2}{\bar{u}^2}}^{q^+} \frac{\mathrm{d}p^+}{p^+} = \int_{r^2}^{\bar{z}^2} \frac{\mathrm{d}\bar{u}^2}{\bar{u}^2} \left(\ln \frac{q^+}{k^+} - \ln \frac{\bar{z}^2}{\bar{u}^2} \right) = Y\rho - \frac{\rho^2}{2}$$

$$Y = \ln \frac{q^+}{k^+}; \qquad \rho = \ln \frac{\bar{z}^2}{r^2}$$

Cancellation of Anti-Time Ordered Diagrams in DLA

Anti-time ordered graphs, involving factors $\frac{p^-}{p^-+k^-} \simeq \Theta(\tau_k - \tau_p)$ are also potentially enhanced by double transverse logs

$$\int_{r^2}^{\bar{z}^2} \frac{\mathrm{d}\bar{u}^2}{\bar{u}^2} \int_{k^+ \frac{\bar{z}^2}{\bar{u}^2}}^{q^+} \frac{\mathrm{d}p^+}{p^+} = \int_{r^2}^{\bar{z}^2} \frac{\mathrm{d}\bar{u}^2}{\bar{u}^2} \ln \frac{\bar{z}^2}{\bar{u}^2} = \frac{\rho^2}{2}$$

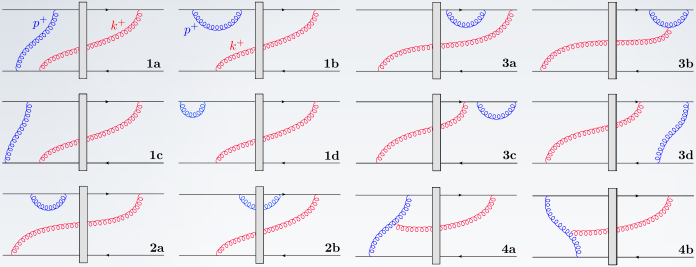

However, double logs cancel in the sum of all ATO diagrams. This also explains the peculiar way double logs arise in [Balitsky & Chirilli '08].

DLA Evolution for the Scattering Amplitude and the Lifetime Ordering Constraint

We conclude that perturbative corrections enhanced by double logarithms $Y\rho$ or ρ^2 can be resummed to all orders by solving a modified DLA equation involving manifest time-ordering

$$\mathcal{A}(q^+, r^2) = \mathcal{A}(0, r^2) + \bar{\alpha}_s \int_{r^2}^{1/Q_0^2} \frac{\mathrm{d}z^2}{z^2} \int_{q_0^+}^{q^+ \frac{r^2}{z^2}} \frac{\mathrm{d}k^+}{k^+} \mathcal{A}(k^+, z^2)$$

As it stands, this equation is non-local in rapidity

$$\partial_Y \mathcal{A}(Y, \rho) = \bar{\alpha}_s \int_0^{\rho} \mathrm{d}\rho_1 \mathcal{A}(Y - \rho + \rho_1, \rho)$$

The Resummed BK Equation

Towards a Resummed Rapidity-Independent Kernel

- By direct iteration of the modified DLA equation, we get

$$\mathcal{A}(Y,\rho) = \int_0^\rho \mathrm{d}\rho_1 f(Y,\rho-\rho_1)\mathcal{A}(0,\rho_1),$$

$$f(Y,\rho) = \delta(\rho) + \Theta(Y-\rho) \underbrace{\sum_{k=1}^{\infty} \frac{\bar{\alpha}_s^k (Y-\rho)^k \rho^{k-1}}{k!(k-1)!}}_{=\sqrt{\frac{\bar{\alpha}_s(Y-\rho)}{\rho}} I_1(2\sqrt{\bar{\alpha}_s(Y-\rho)\rho})}$$

- This can be written in integral representation:
$f(Y,\rho) = \Theta(Y-\rho)\tilde{f}(Y,\rho)$;

$$\tilde{f}(Y,\rho) = \int_{\frac{1}{2}-i\infty}^{\frac{1}{2}+i\infty} \frac{\mathrm{d}\xi}{2\pi i} \exp\left[\frac{\bar{\alpha}_s}{1-\xi}(Y-\rho) + (1-\xi)\rho\right]$$

The Local Kernel in DLA Approximation

A change of variables brings this as usual Mellin representation

$$\tilde{f}(Y,\rho) = \int_{\mathcal{C}} \frac{\mathrm{d}\gamma}{2\pi i} J(\gamma) \exp[\bar{\alpha}_s \chi_{\mathrm{DLA}}(\gamma) Y + (1-\gamma)\rho]$$

$$\bar{\alpha}_s \chi_{\mathrm{DLA}}(\gamma) = \frac{1}{2}\left[-(1-\gamma) + \sqrt{(1-\gamma)^2 + 4\bar{\alpha}_s}\right] = \frac{\bar{\alpha}_s}{(1-\gamma)} - \frac{\bar{\alpha}_s^2}{(1-\gamma)^3} + \cdots$$

$$J(\gamma) = 1 - \bar{\alpha}_s \chi'_{\mathrm{DLA}}(\gamma) = 1 - \frac{\bar{\alpha}_s}{(1-\gamma)^2} + \cdots$$

Mellin representation and exponentiation in Y ensures the existence of an evolution equation for f (and thus for $\mathcal{A}$) with an energy- independent kernel $\mathcal{K}_{\mathrm{DLA}}(\rho)$ defined as inverse Mellin of $\chi_{\mathrm{DLA}}(\gamma)$

$$\tilde{\mathcal{A}}(Y,\rho) = \tilde{\mathcal{A}}(0,\rho) + \bar{\alpha}_s \int_0^Y \mathrm{d}Y_1 \int_0^\rho \mathrm{d}\rho_1 \mathcal{K}_{\mathrm{DLA}}(\rho-\rho_1)\tilde{\mathcal{A}}(Y_1,\rho_1), \quad Y > \rho$$

$$\mathcal{K}_{\mathrm{DLA}}(\rho) = \frac{J_1(2\sqrt{\bar{\alpha}_s \rho^2})}{\sqrt{\bar{\alpha}_s \rho^2}} = 1 - \frac{\bar{\alpha}_s \rho^2}{2} + \frac{(\bar{\alpha}_s \rho^2)^2}{12} + \cdots$$

Coincides with momentum-space kernel proposed by [Sabio Vera '05]; compare with non-local approaches in [Salam '98; Motyka & Staśto '09; Beuf '14].

The Change in the Initial Condition: Impact Factor Resummation

Jacobian of Mellin transform induces also resummation in the initial condition ($\sim$ impact factor):

$$\tilde{\mathcal{A}}(0,\rho) = \int_0^\rho \mathrm{d}\rho_1 \tilde{f}(0,\rho-\rho_1)\mathcal{A}(0,\rho_1),$$
$$\tilde{f}(0,\rho) = \delta(\rho) - \sqrt{\bar{\alpha}_s} J_1(2\sqrt{\bar{\alpha}_s \rho^2}).$$

[$\tilde{\mathcal{A}}(Y,\rho)$ coincides with physical amplitude $\mathcal{A}(Y,\rho)$ for $Y > \rho$]

$$\tilde{\mathcal{A}}(0,\rho) = \begin{cases} \frac{1}{2}\left[1 + \mathrm{J}_0(\bar{\rho})\right] & \text{for} \quad \mathcal{A}(0,\rho) = 1, \\ \frac{\rho}{2}\left[1 + \mathrm{J}_0(\bar{\rho}) + \frac{\pi}{2}\mathbf{H}_0(\bar{\rho})\mathrm{J}_1(\bar{\rho}) - \frac{\pi}{2}\mathbf{H}_1(\bar{\rho})\mathrm{J}_0(\bar{\rho})\right] & \text{for} \quad \mathcal{A}(0,\rho) = \rho, \end{cases}$$

Resummed BFKL/BK Evolution

$$\frac{\partial \tilde{T}_{\boldsymbol{xy}}}{\partial Y} = \int \frac{\mathrm{d}^2\boldsymbol{z}}{2\pi} \bar{\alpha}_s(r_{\min}) \frac{(\boldsymbol{x}-\boldsymbol{y})^2}{(\boldsymbol{x}-\boldsymbol{z})^2(\boldsymbol{z}-\boldsymbol{y})^2} (\tilde{T}_{\boldsymbol{xz}} + \tilde{T}_{\boldsymbol{zy}} - \tilde{T}_{\boldsymbol{xy}} - \tilde{T}_{\boldsymbol{xz}}\tilde{T}_{\boldsymbol{zy}})$$
$$\times \left[\frac{(\boldsymbol{x}-\boldsymbol{y})^2}{\min\{(\boldsymbol{x}-\boldsymbol{z})^2, (\boldsymbol{y}-\boldsymbol{z})^2\}}\right]^{\pm\bar{\alpha}_s A_1} \mathcal{K}_{\mathrm{DLA}}(\bar{\rho}_{\boldsymbol{xyz}})$$

[Iancu, JDM, Mueller, Soyez & Triantafyllopoulos '15]

- Written in terms of a rapidity-independent kernel $\mathcal{K}_{\mathrm{DLA}}(\bar{\rho}(\boldsymbol{x},\boldsymbol{y},\boldsymbol{z})) \equiv \frac{J_1\left(2\sqrt{\bar{\alpha}_s \bar{\rho}^2_{\boldsymbol{xyz}}}\right)}{\sqrt{\bar{\alpha}_s \bar{\rho}^2_{\boldsymbol{xyz}}}}$, as compared to previous strategies [Motyka & Staśto ' 09; Beuf '14] (see also [Sabio Vera '05]).
- Nontrivial resummation involved for the initial condition as well.

Numerical Solution of Resummed BK

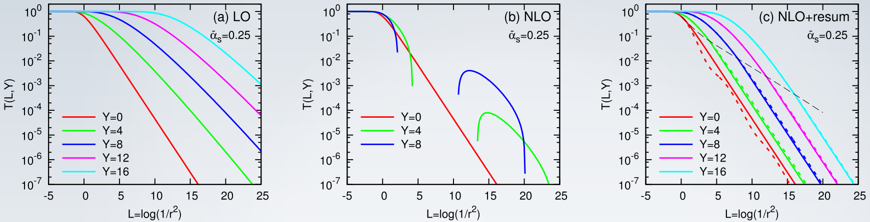

Initial condition of MV type $\mathcal{A}(0,\rho)=1$

Reduction of phase-space coming from time-ordering and giving rise to collinear double logs leads to a considerable reduction in the speed of the evolution

For $\rho > Y$, expected physical behavior $T \propto \mathrm{e}^{-\rho}$

Impact on Phenomenology: Rapidity Dependence of the Saturation Momentum

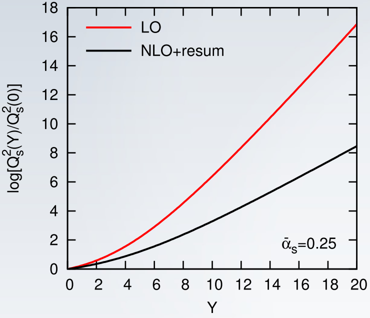

The growth of the saturation scale with Y is considerably reduced by the resummation: for sufficiently large Y, the saturation exponent $\lambda_s \equiv \frac{d\rho_s}{dY}$ smaller by factor 2 compared to LO BFKL (asymptotically, $\lambda_s \sim 0{,}55$).

Including Single Transverse Logarithms

Taking collinear limit $1/Q_s \gg |\boldsymbol{z}-\boldsymbol{x}| \simeq |\boldsymbol{z}-\boldsymbol{y}| \simeq |\boldsymbol{z}-\boldsymbol{u}| \gg |\boldsymbol{u}-\boldsymbol{x}| \simeq |\boldsymbol{u}-\boldsymbol{y}| \gg r \equiv |\boldsymbol{x}-\boldsymbol{y}|$ of NLO BK evolution, one gets

$$\frac{dT(r)}{dY} = \bar{\alpha}_s \int_{r^2}^{1/Q_s^2} \mathrm{d}z^2 \, \frac{r^2}{z^4} \left(1 - \frac{1}{2}\bar{\alpha}_s \ln^2 \frac{z^2}{r^2} - \frac{11}{12}\bar{\alpha}_s \ln \frac{z^2}{r^2}\right) T(z)$$

- ☞ Coefficient $A_1 = 11/12$ of the single log related to DGLAP anomalous dimension: $\gamma(\omega) = \frac{1}{\omega} - A_1 + \mathcal{O}\left(\omega, \frac{N_f}{N_c^3}\right)$
- ☞ Can be taken into account to all orders by shifting the anomalous dimension of the resummed kernel.

The Running Coupling Prescription

Running coupling log is resummed by making $\bar{\alpha}_s \to \bar{\alpha}_s(r^2)$

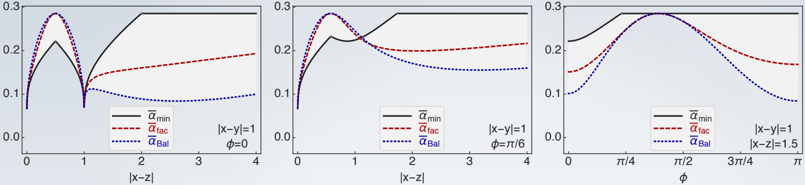

Different prescriptions:

- Smallest Dipole:
$$\bar{\alpha}_{\rm min} = \bar{\alpha}_s(r_{\rm min}), \quad r_{\rm min} = \min\{|\boldsymbol{x}-\boldsymbol{y}|, |\boldsymbol{x}-\boldsymbol{z}|, |\boldsymbol{y}-\boldsymbol{z}|\}$$
- FAC: $\bar{\alpha}_{\rm fac} = \left[\frac{1}{\bar{\alpha}_s(|\boldsymbol{x}-\boldsymbol{y}|)} + \frac{(\boldsymbol{x}-\boldsymbol{z})^2-(\boldsymbol{y}-\boldsymbol{z})^2}{(\boldsymbol{x}-\boldsymbol{y})^2}\frac{\bar{\alpha}_s(|\boldsymbol{x}-\boldsymbol{z}|)-\bar{\alpha}_s(|\boldsymbol{y}-\boldsymbol{z}|)}{\bar{\alpha}_s(|\boldsymbol{x}-\boldsymbol{z}|)\bar{\alpha}_s(|\boldsymbol{y}-\boldsymbol{z}|)}\right]$
- Balitsky: $\bar{\alpha}_{\rm Bal} =$
$$\bar{\alpha}_s(|\boldsymbol{x}-\boldsymbol{y}|)\left[1 + \frac{\bar{\alpha}_s(|\boldsymbol{x}-\boldsymbol{z}|)-\bar{\alpha}_s(|\boldsymbol{y}-\boldsymbol{z}|)}{\bar{\alpha}_s(|\boldsymbol{x}-\boldsymbol{z}|)\bar{\alpha}_s(|\boldsymbol{y}-\boldsymbol{z}|)}\frac{\bar{\alpha}_s(|\boldsymbol{x}-\boldsymbol{z}|)(\boldsymbol{y}-\boldsymbol{z})^2-\bar{\alpha}_s(|\boldsymbol{y}-\boldsymbol{z}|)(\boldsymbol{x}-\boldsymbol{z})^2}{(\boldsymbol{x}-\boldsymbol{z})^2}\right]$$

Fits to HERA Data

Market of Initial Conditions

We get successful fits with two kinds of initial conditions:

☆ Golec-Biernat–Wüsthoff (GBW)

$$T(r,Y_0) = \left\{1 - \exp\left[-\left(\frac{r^2 Q_0^2}{4}\right)^p\right]\right\}^{1/p}$$

☆ Running Coupling McLerran–Venugopalan (rcMV)

$$T(r,Y_0) = \left\{1 - \exp\left[-\left(\frac{r^2 Q_0^2}{4}\bar{\alpha}_s(r)\left[1 + \ln\left(\frac{\bar{\alpha}_{s,\mathrm{sat}}}{\bar{\alpha}_s(r)}\right)\right]\right)^p\right]\right\}^{1/p}$$

The running of the coupling is given by $\alpha_s(r) = \frac{1}{b_{N_f}\ln[4C_\alpha^2/(r^2\Lambda_{N_f}^2)]}$

From Dipole Amplitude to Cross Section: Parameters in the Fit

$$\sigma_{L,T}^{\gamma^* p}(Q^2, x) = 2\pi R_p^2 \sum_f \int \mathrm{d}^2\boldsymbol{r} \int_0^1 \mathrm{d}z |\Psi_{L,T}^{(f)}(\boldsymbol{r}, z; Q^2)|^2 T(\boldsymbol{r}, \ln 1/\tilde{x}_f)$$

$$\sigma_{\mathrm{red}} = \frac{Q^2}{4\pi^2 \alpha_{\mathrm{em}}} \left[\sigma_T^{\gamma^* p} + \frac{2(1-y)}{1+(1-y)^2} \sigma_L^{\gamma^* p} \right]$$

$$\tilde{x}_f = x(1 + 4m_f^2/Q^2) \ \ (\text{we take } \tilde{x}_c < 0{,}01); \qquad F_L = \frac{Q^2}{4\pi^2 \alpha_{\mathrm{em}}} \sigma_L^{\gamma^* p}$$

• 3 light quarks and charm all treated on the same footing (good fits for $m_{u,d,s} = 50 - 140$ MeV and $m_c = 1{,}3 - 1{,}4$ GeV)

Just 4 free parameters:

- R_p: proton radius
- Q_0: target's inverse transverse size
- p: steepness of the amplitude towards saturation
- C_α: fudge factor in the running coupling

How the Fits Look Like

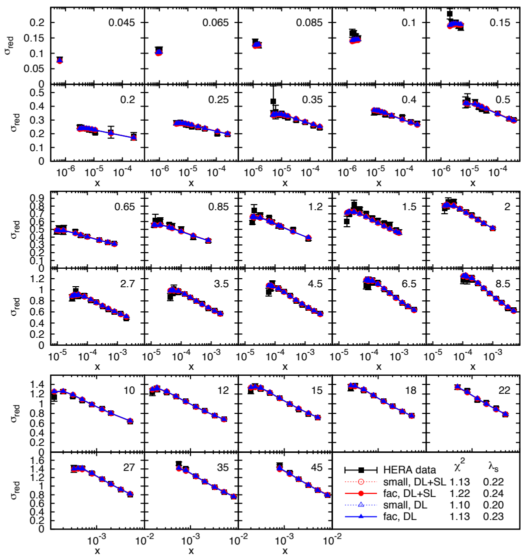

How the Fits Look Like

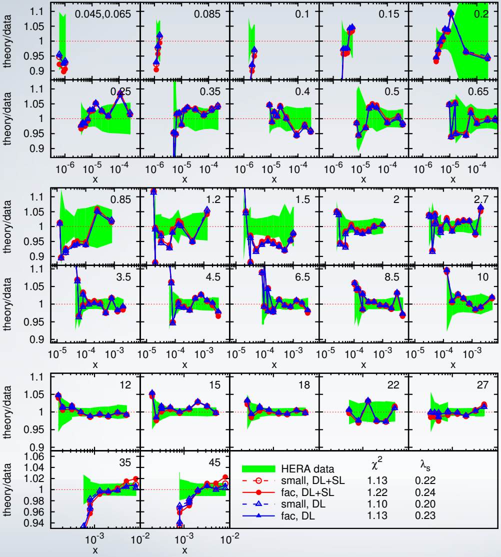

How the Fits Look Like

init cdt.	RC schm	sing. logs	χ^2 per data point			parameters			
			$\sigma_{\rm red}$	$\sigma_{\rm red}^{c\bar{c}}$	F_L	R_p[fm]	Q_0[GeV]	C_α	p
GBW	small	yes	1.135	0.552	0.596	0.699	0.428	2.358	2.802
GBW	fac	yes	1.262	0.626	0.602	0.671	0.460	0.479	1.148
rcMV	small	yes	1.126	0.565	0.592	0.707	0.633	2.586	0.807
rcMV	fac	yes	1.228	0.647	0.594	0.677	0.621	0.504	0.541
GBW	small	no	1.121	0.597	0.597	0.716	0.414	6.428	4.000
GBW	fac	no	1.164	0.609	0.594	0.697	0.429	1.195	4.000
rcMV	small	no	1.093	0.539	0.594	0.718	0.647	7.012	1.061
rcMV	fac	no	1.132	0.550	0.591	0.699	0.604	1.295	0.820

init cdt.	RC schm	sing. logs	χ^2/npts for $Q^2_{\rm max}$			
			50	100	200	400
GBW	small	yes	1.135	1.172	1.355	1.537
GBW	fac	yes	1.262	1.360	1.654	1.899
rcMV	small	yes	1.126	1.170	1.182	1.197
rcMV	fac	yes	1.228	1.304	1.377	1.421
GBW	small	no	1.121	1.131	1.317	1.487
GBW	fac	no	1.164	1.203	1.421	1.622
rcMV	small	no	1.093	1.116	1.106	1.109
rcMV	fac	no	1.131	1.181	1.171	1.171

What the Fit Tells Us

- Very good quality fits for the most recent HERA data (H1+ZEUS combined analysis) for $\sigma_{\text{red}}^{\gamma^* p}$: χ^2 per point $\sim$ 1.1-1.2
- Very discriminatory

Favors 🙂	Disfavors 🙁
rcMV initial condition (pQCD + saturation)	fixed-coupling MV and GBW (at high Q^2) initial conditions
physical prescriptions for running (FAC, smallest dipole)	Balitsky prescription for RC
physical values of fit parameters	anomalous dimension >1

Conclusions and Outlook

Summary

- In the LHC, very low values of x will be probed in pp, pA and AA collisions, providing a great opportunity to understand the high-energy dynamics of strong interactions.
- Our study assembles for the first time all the important contributions to high-energy QCD evolution: rapidity/energy logs, collinear double and single logs, running coupling and saturation

Summary

- In the LHC, very low values of x will be probed in pp, pA and AA collisions, providing a great opportunity to understand the high-energy dynamics of strong interactions.
- Our study assembles for the first time all the important contributions to high-energy QCD evolution: rapidity/energy logs, collinear double and single logs, running coupling and saturation
- We identified the diagrammatic origin of double transverse logs and show how to resum them into a local kernel

Summary

- In the LHC, very low values of x will be probed in pp, pA and AA collisions, providing a great opportunity to understand the high-energy dynamics of strong interactions.
- Our study assembles for the first time all the important contributions to high-energy QCD evolution: rapidity/energy logs, collinear double and single logs, running coupling and saturation
- We identified the diagrammatic origin of double transverse logs and show how to resum them into a local kernel
- We provided very solid and discriminatory fits to high-precision DIS data

Summary

- In the LHC, very low values of x will be probed in pp, pA and AA collisions, providing a great opportunity to understand the high-energy dynamics of strong interactions.
- Our study assembles for the first time all the important contributions to high-energy QCD evolution: rapidity/energy logs, collinear double and single logs, running coupling and saturation
- We identified the diagrammatic origin of double transverse logs and show how to resum them into a local kernel
- We provided very solid and discriminatory fits to high-precision DIS data

What Next?

1. Double Logs in an Arbitrary Frame: Symmetric $\gamma^*\gamma^*$ Scattering
2. Introduce Energy-Momentum Conservation $(\gamma(\omega = 1) = 0)$
3. Resummation of Impact Factor in $k_\perp$ Factorization
4. Collinear Resummation in Inclusive Forward Hadron Production

   [Staśto, Xiao & Zaslavsky'13; Altinoluk, Armesto, Beuf, Kovner & Lublinsky'14]
5. Adding Pure NLO Terms in BK Equation
6. Performing Full Matching with DGLAP
7. Use of the Extracted Dipole Amplitude in Processes Like: particle multiplicity in hadronic collisions, the diffractive structure functions, the elastic production of vector mesons, or the forward particle production in heavy-ion collisions

Back-Up Slides

Collinear Resummation à la Salam

Double Mellin Representation for BFKL Green's function

$$G(k, k_0, Y) = \frac{1}{k^2} \int_{a-i\infty}^{a+i\infty} \frac{\mathrm{d}\omega}{2\pi i} \int_{\frac{1}{2}-i\infty}^{\frac{1}{2}+i\infty} \frac{\mathrm{d}\gamma}{2\pi i} \left(\frac{s}{k k_0}\right)^{\omega} \mathrm{e}^{\gamma\rho} \frac{1}{\omega - \kappa(\omega, \gamma)},$$

$$\rho = \ln(k^2/k_0^2); \qquad \kappa(\omega,\gamma) = \bar{\alpha}_s \chi(\gamma) + \bar{\alpha}_s^2 \chi_1(\omega,\gamma) + \cdots$$

Matching with DGLAP through identification of relevant evolution variable for $k^2 > k_0^2$ and viceversa: ω-shift

$$G(k, k_0, Y) = \frac{1}{k^2} \int_{a-i\infty}^{a+i\infty} \frac{\mathrm{d}\omega}{2\pi i} \int_{\frac{1}{2}-i\infty}^{\frac{1}{2}+i\infty} \frac{\mathrm{d}\gamma}{2\pi i} \left(\frac{s}{k^2}\right)^{\omega} \mathrm{e}^{(\gamma+\omega/2)\rho} \frac{1}{\omega - \kappa(\gamma, \omega)}$$

$$= \frac{1}{k_0^2} \int_{a-i\infty}^{a+i\infty} \frac{\mathrm{d}\omega}{2\pi i} \int_{\frac{1}{2}-i\infty}^{\frac{1}{2}+i\infty} \frac{\mathrm{d}\gamma}{2\pi i} \left(\frac{s}{k_0^2}\right)^{\omega} \mathrm{e}^{(1-\gamma+\omega/2)(-\rho)} \frac{1}{\omega - \kappa(\omega, \gamma)}$$

Dipole Scattering Amplitude

Glauber-Mueller Formula for Dipole S-Matrix

$$S(r,Y) = \exp\left[-\frac{r^2 Q_s^2(Y)}{4}\right]$$

$(T(r) \sim 1$ for $r \gg \frac{1}{Q_s}$ (black disk limit); $T(r) \sim 0$ for $r \ll \frac{1}{Q_s}$ (color transparency)

GBW Model for Dipole Cross Section

$$\sigma^{\rm dip} = \sigma_0 \left[1 - \exp\left(-\frac{r^2 Q_s^2(x)}{4}\right)\right]; \quad Q_s^2(x) = Q_0^2 \left(\frac{x_0}{x}\right)^{\lambda}$$

AAMQS Parametrization

$$T(r,b) = 1 - \exp\left[-\frac{(r^2 Q_{s0}^2(b))^{\gamma}}{4} \ln\left(\frac{1}{\Lambda r} + e\right)\right]$$

Saturation Momentum

Gribov-Levin-Ryskin Estimate

$$Q_s \sim \alpha_s^2 \Lambda_{\mathrm{QCD}} \left(\frac{1}{x}\right)^{\alpha_P - 1}$$

DLA Estimate of Rapidity Dependence of Dipole Scattering Amplitude $(r \ll 1/Q_{s0})$

$$T(r, Y) \sim (rQ_{s0})^2 (\bar{\alpha}_s Y)^{1/4} \rho^{-3/4} \exp[2\sqrt{2\bar{\alpha}_s Y \rho}]$$

BFKL Green's Function, Dipole Amplitude and Unintegrated Gluon Distribution

$$
\begin{aligned}
T^{Y}_{\boldsymbol{r}_1\boldsymbol{r}_2} &= \int \mathrm{d}^2\boldsymbol{r}'_1 \mathrm{d}^2\boldsymbol{r}'_2 \tilde{\mathcal{G}}(\boldsymbol{r}_1,\boldsymbol{r}_2;\boldsymbol{r}'_1,\boldsymbol{r}'_2;Y)\mathrm{e}^{-\mathrm{i}\boldsymbol{q}\cdot\frac{(\boldsymbol{r}'_1+\boldsymbol{r}'_2)}{2}} \\
&= \int \frac{\mathrm{d}^2\boldsymbol{k}}{(2\pi)^2}(1-\mathrm{e}^{\mathrm{i}\boldsymbol{k}\cdot\boldsymbol{r}_{01}})\tilde{T}^{Y}(\boldsymbol{k}) \qquad (\boldsymbol{q}=0) \\
\alpha_s(k^2)\phi(k,Y) &= \frac{N_c S_\perp}{(2\pi)^3}k^2\tilde{T}^{Y}(\boldsymbol{k}) \\
\tilde{\mathcal{G}}(\boldsymbol{r}_1,\boldsymbol{r}_2;\boldsymbol{r}'_1,\boldsymbol{r}'_2;Y) &= \int \mathrm{d}^2\boldsymbol{k}\mathrm{d}^2\boldsymbol{k}'\mathrm{e}^{\mathrm{i}\boldsymbol{k}\cdot\boldsymbol{r}_{12}}\mathrm{e}^{\mathrm{i}\boldsymbol{k}\cdot(\boldsymbol{r}_{12}-\boldsymbol{r}_{1'2'})} \\
&\times (1-\mathrm{e}^{-\mathrm{i}(\boldsymbol{k}+\boldsymbol{q}/2)\cdot\boldsymbol{r}_{12}})(1-\mathrm{e}^{\mathrm{i}(-\boldsymbol{k}+\boldsymbol{q}/2)\cdot\boldsymbol{r}_{12}}) \\
&\times G(\boldsymbol{k}+\boldsymbol{q}/2,-\boldsymbol{k}+\boldsymbol{q}/2;\boldsymbol{k}'+\boldsymbol{q}/2,-\boldsymbol{k}'+\boldsymbol{q}/2;Y) \\
&\times (1-\mathrm{e}^{\mathrm{i}(\boldsymbol{k}+\boldsymbol{q}/2)\cdot\boldsymbol{r}_{1'2'}})(1-\mathrm{e}^{-\mathrm{i}(-\boldsymbol{k}+\boldsymbol{q}/2)\cdot\boldsymbol{r}_{1'2'}})
\end{aligned}
$$

Completing DLA to BFKL/BK Evolution

We can now easily promote our local DLA equation to easily include NLL BFKL/BK:

1. $\tilde{T}(Y,\rho) = \mathrm{e}^{-\rho}\tilde{\mathcal{A}}(\mathrm{Y},\rho)$
2. Return to transverse coordinates: $\rho = \ln(1/r^2Q_0^2)$; $\rho - \rho_1 = \ln(z^2/r^2)$; $\tilde{T}(Y,\rho) = \tilde{T}_{\boldsymbol{xy}}(Y)$; $2\tilde{T}(Y,z^2) \to \tilde{T}_{\boldsymbol{xz}}(Y) + \tilde{T}_{\boldsymbol{zy}}(Y)$
3. Restore full dipole kernel $\frac{r^2}{z^4}\mathrm{d}z^2 \to \frac{1}{\pi}\mathcal{M}_{\boldsymbol{xyz}}\mathrm{d}^2\boldsymbol{z}$
4. Introduce the virtual term and temove IR and UV cutoffs in the $\boldsymbol{z}$ integration
5. Replace the argument of $\mathcal{K}_{\mathrm{DLA}}$ by $\ln\frac{z^2}{r^2} \to \sqrt{L_{\boldsymbol{xzr}}L_{\boldsymbol{yzr}}}$, with $L_{\boldsymbol{xzr}} \equiv \ln[(\boldsymbol{x}-\boldsymbol{z})^2/(\boldsymbol{x}-\boldsymbol{y})^2]$